

---

Masters Theses

Student Theses and Dissertations

---

1968

## Kinetics of the formation of strontium zirconate

W. H. Parker

Follow this and additional works at: [https://scholarsmine.mst.edu/masters\\_theses](https://scholarsmine.mst.edu/masters_theses)



Part of the [Ceramic Materials Commons](#)

Department:

---

### Recommended Citation

Parker, W. H., "Kinetics of the formation of strontium zirconate" (1968). *Masters Theses*. 6880.  
[https://scholarsmine.mst.edu/masters\\_theses/6880](https://scholarsmine.mst.edu/masters_theses/6880)

This thesis is brought to you by Scholars' Mine, a service of the Missouri S&T Library and Learning Resources. This work is protected by U. S. Copyright Law. Unauthorized use including reproduction for redistribution requires the permission of the copyright holder. For more information, please contact [scholarsmine@mst.edu](mailto:scholarsmine@mst.edu).

90  
152  
✓

KINETICS OF THE FORMATION  
OF STRONTIUM ZIRCONATE

BY  
WILLIAM HENRY PARKER - 1941

---

A  
THESIS  
submitted to the faculty of  
THE UNIVERSITY OF MISSOURI - ROLLA  
in partial fulfillment of the requirements for the  
Degree of  
MASTER OF SCIENCE IN CERAMIC ENGINEERING  
Rolla, Missouri  
1968

---

132094

Approved by

Robert E. Moore      Anders Levick  
Albert E. Boston      \_\_\_\_\_

## ABSTRACT

The decomposition rate of strontium carbonate ( $\text{SrCO}_3$ ) was measured using a TGA apparatus. It was found to deviate slightly from zero order classical reaction. The rate of formation of strontium zirconate ( $\text{SrZrO}_3$ ) from zirconium oxide ( $\text{ZrO}_2$ ) and strontium oxide ( $\text{SrO}$ ) in the form of the decomposition product of  $\text{SrCO}_3$  was measured using quantitative x-ray diffraction for mineralogical analysis. It was found to most nearly follow the Zhuravlev-Lesokhin-Tempel' man rate equation. The rate of decomposition of strontium carbonate was found to be more rapid than the rate of formation of strontium zirconate such that for the most part strontium oxide is reacting with the zirconium oxide. The activation energies for the decomposition of strontium carbonate and the formation of strontium zirconate from zirconium oxide and the decomposition product of strontium carbonate were calculated to be  $50.6 \pm 2.6$  kilocalories per mole and  $81.3 \pm 9.7$  kilocalories per mole, respectively. The Hedvall effect was observed in the rate of formation of strontium zirconate at the transformation temperature of zirconium oxide.

DEDICATION

TO THE MEMORY OF:

Dr. Donald L. Branson

1940 - 1967

## ACKNOWLEDGMENTS

The author wishes to acknowledge the help and inspiration of Dr. Donald L. Branson without whose aid this work would never have been undertaken and whose untimely death deprived him of being able to see it to its completion. The author also wishes to thank Dr. Robert E. Moore for his help and suggestions and Mr. Timothy L. Clancy for his aid in the experimental techniques.

The financial support of Kaiser Refractories was most valuable and appreciated.

## TABLE OF CONTENTS

	Page
LIST OF FIGURES . . . . .	vi
I. INTRODUCTION . . . . .	1
II. LITERATURE SURVEY . . . . .	3
III. PROCEDURE . . . . .	11
IV. RESULTS . . . . .	16
V. DISCUSSION OF RESULTS . . . . .	31
VI. CONCLUSIONS . . . . .	36
VII. SUGGESTIONS FOR FUTURE WORK . . . . .	37
BIBLIOGRAPHY . . . . .	38
APPENDIX A - X-RAY DIFFRACTION CALIBRATION CURVE . . . . .	41
APPENDIX B - ANALYSIS OF VARIANCE OF LINEAR REGRESSION OF ARRHENIUS PLOT FOR DECOMPOSITION OF STRONTIUM CARBONATE . . . . .	42
APPENDIX C - ANALYSIS OF VARIANCE OF LINEAR REGRESSION OF ARRHENIUS PLOT FOR FORMATION OF STRONTIUM ZIRCONATE	43
APPENDIX D - ELECTRON PHOTOMICROGRAPHS OF REACTED POWDERS . . . . .	44
APPENDIX E - DIFFERENTIAL THERMAL ANALYSIS FIGURES . . . . .	45
VITA . . . . .	46

## LIST OF FIGURES

<u>Figures</u>	Page
1. TGA Assembly .....	12
2. Fraction SrCO <sub>3</sub> Decomposed Versus Time .....	17
3. Arrhenius Plot of SrCO <sub>3</sub> Decomposition .....	19
4. Fraction SrZrO <sub>3</sub> Formation Versus Time .....	20
5. Ln Rate Constant Versus Fraction Reaction Completed at 1100 <sup>o</sup> C	23
6. Ln Rate Constant Versus Fraction Reaction Completed at 1100 <sup>o</sup> C	24
7. Ln Rate Constant Versus Fraction Reaction Completed at 1150 <sup>o</sup> C	25
8. Ln Rate Constant Versus Fraction Reaction Completed at 1150 <sup>o</sup> C	26
9. Ln Rate Constant Versus Fraction Reaction Completed at 1200 <sup>o</sup> C	27
10. Ln Rate Constant Versus Fraction Reaction Completed at 1200 <sup>o</sup> C	28
11. Arrhenius Plot of SrZrO <sub>3</sub> Formation .....	30
A-1 X-Ray Diffraction Calibration Curve .....	41
D-1 Electron Photomicrographs of Reacted Powders .....	44
E-1 DTA Plots .....	45

Tables

1. Slope of Plot of Ln Fraction SrCO <sub>3</sub> Decomposed versus Ln Time	18
2. Calculated Rate Constants .....	21

## I. INTRODUCTION

The solid state reaction between strontium carbonate ( $\text{SrCO}_3$ ) and zirconium oxide ( $\text{ZrO}_2$ ) as raw materials, was examined in an attempt to gain a better understanding of solid state reactions in general and especially those in which one of the reactants decomposes such that one of its decomposition products is gaseous. To accomplish this objective, the kinetics of this reaction were studied with special attention to:

1. The rate equation which best fits the experimental data, i. e. the fraction completion of the reaction versus time.
2. The mechanism of the reaction: (a) whether the reaction is phase-boundary or transport controlled, (b) whether the geometry of the mechanism of the reaction is nuclei growth (spatial) or diffusion through a continuous product layer (spherical shell), (c) whether the reaction is between the original reactants or between  $\text{ZrO}_2$  and  $\text{SrO}$  resulting from the decomposition of  $\text{SrCO}_3$ .
3. The effect of the inversion of  $\text{ZrO}_2$  on the rate of the reaction, i. e. the Hedvall effect.
4. The effect of the inversion of  $\text{ZrO}_2$  on the mechanism of the reaction.

There are many obstacles involved in making a kinetic study of even the most simple solid state reactions. The most significant barrier to obtaining satisfactory rate data of most solid state reactions is in the analysis of the products. This difficulty results because conventional solvent and chemical



separation techniques are not applicable since the ratio between most elements is constant before, during, and after the reaction. It was anticipated that the reaction could be followed by monitoring the weight lost through CO<sub>2</sub> evolution. Since this was not possible, quantitative analysis was determined by x-ray diffraction techniques.

This particular reaction was chosen because of interest in strontium zirconate due to plastic deformation behavior at room temperature and its perovskite structure and related properties.

## II. LITERATURE SURVEY

The step controlling the rate of a solid state reaction is usually either the chemical combination at the reaction interface or the transport of reactants to the reaction zone. In a diffusion-controlled reaction, assuming only plane surfaces, uni-directional diffusional processes and constant diffusion coefficients, the product layer thickness ( $y$ ) is related to reaction time ( $t$ ) by the widely known parabolic rate law,

$$y^2 = 2kDt \quad (1)$$

where ( $k$ ) is a proportionality constant and ( $D$ ) is the diffusion coefficient of the migrating species.

Since most ceramic processes are carried out on intimately mixed ceramic powders, the planar surface criterion is not usually met. Jander<sup>1</sup> in 1927 developed a rate equation for powdered compacts from the planar interface parabolic rate law. Jander's model is based upon the following assumptions:

1. The reaction can be considered as an additive reaction, i. e. two reactants forming one product.
2. Nucleation, followed by surface diffusion, occurs at a temperature below that needed for bulk diffusion so that a coherent product layer is present when bulk diffusion does occur.
3. The chemical reaction at the phase boundary is sufficiently more rapid than the transport process so that the reaction is bulk diffusion controlled.

4. Bulk diffusion is uni-directional.
5. The product is not miscible with any of the reactants.
6. The reactants are spherical particles of uniform radii.
7. The ratio of the volume of the products to the volume of the reactants is one.
8. The increase in the thickness of the product layer follows the parabolic rate law (Equation 1).
9. The diffusion coefficient of the diffusing species is not a function of time.
10. The thermodynamic activity of reactants remains constant on both sides of the reaction interface.

Letting  $(V)$  denote the volume of material still unreacted at time  $(t)$

then

$$V = \frac{4}{3} \pi (r - y)^3 \quad (2)$$

where  $(r)$  is the initial radius of the reacting particle. Letting  $(x)$  be the fractional completion of reactions at time  $(t)$ , the volume of unreacted material is also given by

$$V = \frac{4}{3} \pi r^3 (1 - x) \quad (3)$$

Equations (2) and (3) can be equated to yield

$$y = r [1 - (1 - x)^{1/3}] \quad (4)$$

Combining Equations (4) and (1) and rearranging yields

$$k_J t = \frac{2kDt}{r^2} = [1 - (1 - x)^{1/3}]^2 \quad (5)$$

This Equation (5) is the widely known Jander equation which relates the fraction of reaction completed to time where  $k_J$  is the rate constant for the Jander equation. In order to determine the rate constant for an isothermal Jander solid state reaction, the fraction reacted must be determined as a function of time and a plot of  $[1 - (1 - x)^{1/3}]^2$  versus time made. This plot should give a straight line whose slope is the rate constant ( $k_J$ ). If the Jander model applies to the system being studied, the rate constant should not drift as the reaction proceeds. If the rate constant does drift, another model must be sought. Since the Jander model requires a number of ideal situations, it is often found that a more complicated situation actually exists.

Kroger and Ziegler<sup>2,3</sup> indicated that Jander's assumption of a constant diffusion coefficient was not applicable to all solid state systems, particularly during the early stages of reaction. Kroger and Ziegler used Jander's geometry (Jander's assumptions 1 - 7) and assumed that the diffusion coefficient of the transported species was inversely proportional to time. Equation (6) is the Kroger-Ziegler Equation.

$$k_{K-Z} \ln t = \frac{2k}{r} \ln t = [1 - (1 - x)^{1/3}]^2 \quad (6)$$

To determine the Kroger-Ziegler rate constant ( $k_{K-Z}$ ), the slope of a plot of  $[1 - (1 - x)^{1/3}]^2$  versus  $\log_e$  time is used.

Zhuravlev, Lesokhin, and Tempel'man<sup>4</sup> modified the Jander equation by assuming that the activity of the reacting substances was proportional to the fraction of unreacted material ( $1 - x$ ). Their relationship between

fraction of reaction completed and time is given by Equation (7).

$$k_{Z-L-T}t = \left[ \left( \frac{1}{1-x} \right)^{1/3} - 1 \right]^2 \quad (7)$$

Ginstling and Brounshtein<sup>5</sup> arrived at a model using Jander's assumptions with the exception of the parabolic rate law. They indicated that the parabolic rate law asserted that the reaction surface area remained constant. However, when they considered spherical particles, this surface actually decreased in area as the reaction proceeded. They discarded the parabolic rate law in favor of an equation relating the growth of the product layer to Barrer's<sup>6</sup> equation for steady state heat transfer through a spherical shell. Equation (8) is the Ginstling-Brounshtein Equation.

$$k_{G-B}t = \frac{2kDt}{r} = 1 - 2/3x - (1-x)^{2/3} \quad (8)$$

Carter<sup>7,8</sup> further improved the Ginstling-Brounshtein model by accounting for differences in the volume of the product layer with respect to that of the reactants. Carter also used Barrer's equation to represent the rate of product formation and entered a (Z) term to account for the change in volume, where (Z) represents the volume of the reaction product formed per unit volume of the reactant consumed. Valensi<sup>9</sup> earlier developed, mathematically, the same solid reaction model from a different starting point. Thus, Equation (9) is referred to as the Valensi-Carter equation.

$$k_{V-C}t = \frac{2ktD}{r} = \frac{Z - [1 + (Z-1)x]^{2/3} - (Z-1)(1-x)^{2/3}}{Z-1} \quad (9)$$

Dunwald-Wagner<sup>10</sup> derived an equation for solid state reaction analysis based on a solution to Fick's second law for diffusion into or out of a sphere. Serin and Ellickson<sup>11</sup> expressed the Dunwald-Wagner equation in terms of the fractional completion of the reaction as in Equation (10).

$$k_{D-W}t = \frac{\pi^2 Dt}{r^2} = \ln \frac{6}{\pi^2 (1-x)} \quad (10)$$

Although all the models discussed thus far are limited by the criterion of only spherical particles of the same radius taking part in the reaction, they have been shown to represent many solid state reactions<sup>12,13,14</sup>. There have been attempts to introduce particle size distribution into a workable model. However, these have resulted in models that involve complicated mathematics and contain parameters which are difficult to measure. Models including particle size distribution have been developed by Miyagi<sup>15</sup> (based on Jander's assumptions), Sasaki<sup>16</sup> (based on Carter's assumptions), and Gallagher<sup>17</sup> (based on Dunwald-Wagner's assumptions).

In the case where the reaction starts only at the contact zones between particles and the reaction proceeds by diffusion through the contact zones, Jander's assumption that the surface of one component is completely and continuously covered with particles of the other component is obviously not valid. To take into consideration the effect of the number of contact points, Komotsu<sup>18</sup> introduced into the Jander equation the mixing ratio of the two components, the radii of the two components, and a parameter which describes the packing state of the powders.

The solid state reaction models for powdered compacts thus far described have been based on the assumption that, initially, surface diffusion is so rapid that the surface of the reacting particle is rapidly coated with a continuous product layer. The subsequent reaction rate is taken to be the rate of inward diffusional growth from this product shell. There is another way of looking at the initial product formation and subsequent growth. This approach takes into consideration the nucleation of products at active sites and the rate at which the nucleated particles grow. According to Welch,<sup>19</sup> such a mechanism is possible whenever the product phase is partially miscible in one of the reactants.

There is increasing interest in the nuclei growth mechanisms and many mathematical models (Jacobs-Thompkins,<sup>20</sup> Fine,<sup>21</sup> Avrami,<sup>22,23,24</sup> Erofe'ev,<sup>25</sup> Christian<sup>26</sup>) have been advanced relating nucleation and nuclei growth rates to the kinetics of solid state reactions. The general form of the kinetic equations for nuclei growth models is as follows:

$$(k_n t)^m = \ln \frac{1}{1-x} \quad (11)$$

where (m) is a parameter which is a function of (a) reaction mechanism, (b) number of nuclei present, (c) compositions of parent and product phases, and (d) geometry of the nuclei. Christian<sup>26</sup> has summarized the values of (m) which may be obtained for various boundary conditions. If a solid state reaction can be represented by a nuclei growth model, according to Equation (11), a plot of  $\ln \ln \frac{1}{1-x}$  versus  $\ln t$  (nuclei growth analysis) should yield a straight line with slope (m) and intercept (m ln k).

When diffusion through the product layer is so rapid that the reactants cannot combine fast enough at the reaction interface to establish equilibrium, the solid state reaction is said to be phase-boundary controlled. The product layer is discontinuous when the molar volume of the product is considerably different from that of the reactant upon which it is growing. According to Laidler,<sup>27</sup> when a discontinuous product phase occurs, the rate determining step may be the chemical process occurring at the phase boundary. Under these circumstances, the rate is determined by the available interface area and the process is referred to as topochemical.

Equations relating  $(x)$  and  $(t)$  have been derived for simple geometrical systems assuming (a) the reaction rate is phase-boundary controlled, (b) the reaction rate is proportional to the surface area of the fraction of unreacted material, and (c) the nucleation step occurs virtually instantaneously, so that the surface of each particle is covered with a layer of product. The models developed from the foregoing boundary conditions are called phase-boundary or contracting-volume models. For a sphere reacting from the surface inward,<sup>28</sup> the rate equation is

$$k_{\text{PB-S}} t = \frac{u}{r} t = 1 - (1 - x)^{1/3} \quad (12)$$

and for a circular disc or a cylinder reacting from the edge inward<sup>28</sup>

$$k_{\text{PB-D}} t = \frac{u}{r} t = 1 - (1 - x)^{1/2} \quad (13)$$

where  $(u)$  is the velocity at which the interface advances into the particle.



Note that for phase boundary reactions the rate constant is proportional to the inverse of the radius where for transport controlled reactions the rate constant is proportional to the inverse of the square of the radius.

Equations analogous to classical rate equations have often been applied to solid state reactions. The integrated form of the general kinetic equation based on the concept of an order of reaction is

$$k_c t = \frac{1}{n-1} \left[ \frac{1}{(1-x)^{n-1}} - 1 \right] \quad (14)$$

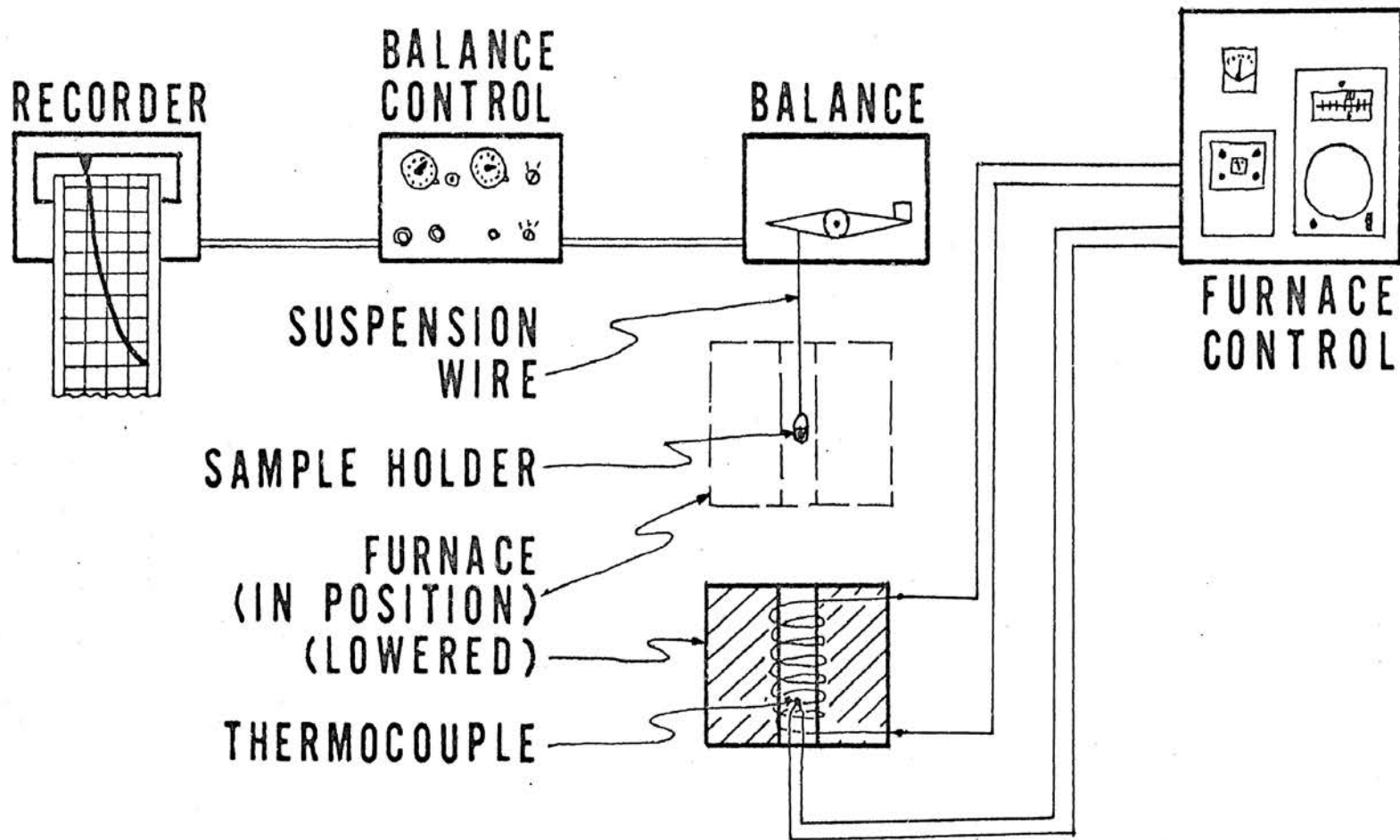
where (n) is the order of the reaction. For certain values of (n), Equation (14) leads to some of the equations based upon physical models. When  $n = 2/3$ , Equation (14) is identical to Equation (12). Likewise when  $n = 1/2$ , Equation (14) is identical to Equation (13). When the rate determining step is nucleation and there is an equal probability of nucleation on each active site, one obtains a kinetic equation of the first-order.<sup>29</sup> Whenever the rate of reaction is proportional to the volume of unreacted material present, it is, according to classical kinetics, a first order reaction. At present, values of (n), other than 1/2, 2/3, or 1, lead to equations with no obvious physical significance.

### III. PROCEDURE

The materials used in this work were Reagent Grade Strontium Carbonate from Allied Chemical Company and Purified Zirconium Oxide from Fisher Scientific Company.

In determining the rate of decomposition of the strontium carbonate, the as-received powder was placed in a small platinum boat and suspended with nichrome wire from a Cahn RG recording electrobalance. The electrobalance was connected to a Texas Instruments Servo/Riter II Recorder with a range of one millivolt full scale. The furnace used was a Kanthal-wound vertical tube furnace controlled by a West Gardsman on-off controller using a platinum-platinum 13% rhodium thermocouple. Figure 1 shows the arrangement of the equipment in this thermo-gravimetric analysis assembly. A sample size of 168 milligrams was used so that, with the balance set at 50 milligrams full scale, per cent decomposed could be read directly on the recorder chart. The furnace was set at the desired temperature and allowed to hold at temperature for at least one-half hour before each run. When a run was started, the furnace was raised around the sample, simultaneous with starting the recorder; a record of weight loss (equivalent to per cent decomposed) versus time was thus obtained.

For the determinations of rate of formation of strontium zirconate, the as-received strontium carbonate and zirconium oxide were wet-mixed with acetone and DuPont Duco Cement. The mixing was continued until the acetone evaporated and the mixture formed small granules. The mixture was then



# TGA ASSEMBLY

Figure 1

pressed into pellets of approximately one gram using 12,000 pounds force on a half-inch diameter die. The pellets were heated overnight at 350°C to burn out the Duco Cement binder. The samples were then fired in a Hevi-duty muffled box-type glo-bar furnace. The furnace was controlled by the same West Gardsman controller as was used earlier. During firing, the samples rested on pieces of platinum foil. The samples were analyzed using quantitative x-ray<sup>30</sup> diffraction methods on a General Electric XRD 5 diffractometer. For this analysis the (321) strontium zirconate line was used because it is furthest removed from any strontium carbonate and zirconia lines. To minimize the effect of hygroscopic behavior of the strontium oxide changing the volume of the samples, collodion was used as a binder in x-ray specimens. The calibration curve for the quantitative x-ray diffraction determinations appears in Appendix A. The standards used for this calibration were mechanical mixtures of SrO, ZrO<sub>2</sub> and SrZrO<sub>3</sub>. From the calibration curve, this method should give values for fraction SrZrO<sub>3</sub> within at least  $\pm 0.05$  for similarly prepared samples. The value for fraction SrZrO<sub>3</sub> should also be the value of fraction reaction completed; however, because of the possible effect the stabilized zirconia might have on this quantitative x-ray diffraction method, this technique and calibration curve may not be completely valid. It does, however, appear to be better than other methods available. A wet chemical separation technique involving the dissolving of unreacted SrO by dilute HCl was tried but was found to be inapplicable because of the leaching of strontium ions from the extremely fine particles of SrZrO<sub>3</sub> with their large surface area.

Electron probe microanalysis and optical microscopy did not appear to be good techniques for this application because of the inherent problems involved in preparing polished sections of slightly sintered samples for observation with the electron probe or optical microscope and the problem of getting a large enough sample size of small powders for observation and the problem of distinguishing between these powders. Because of the shift in the zirconia peak caused by the stabilization by the strontia and the hygroscopic behavior of the strontium oxide, the strontium zirconate peaks alone were used in the analysis.

For observing the reaction by differential thermal analysis techniques, an R. L. Stone Differential Thermal Analysis Apparatus was used with "micro-sample" sample holders. Ten degrees centigrade per minute was used as the heating rate for all runs. The runs were made using the mixture of strontium carbonate and zirconium oxide versus an alumina standard as well as zirconium oxide, and strontium carbonate as the reference materials. The use of the latter two was to try to mask the effect changes in these components had on the DTA curves.

Transmission electron photomicrographs of the reacted powders were made using a Hitachi HU11A Electron Microscope. The samples were prepared by depositing them from a water slurry onto a collodion coated copper grid. The thin film of collodion had been coated on the copper grid by the spread film method. This was accomplished by allowing a drop of a collodion-amyl acetate solution to spread and dry while floating on the surface of a dish of water. A glass slide on which the grids were resting was then raised from

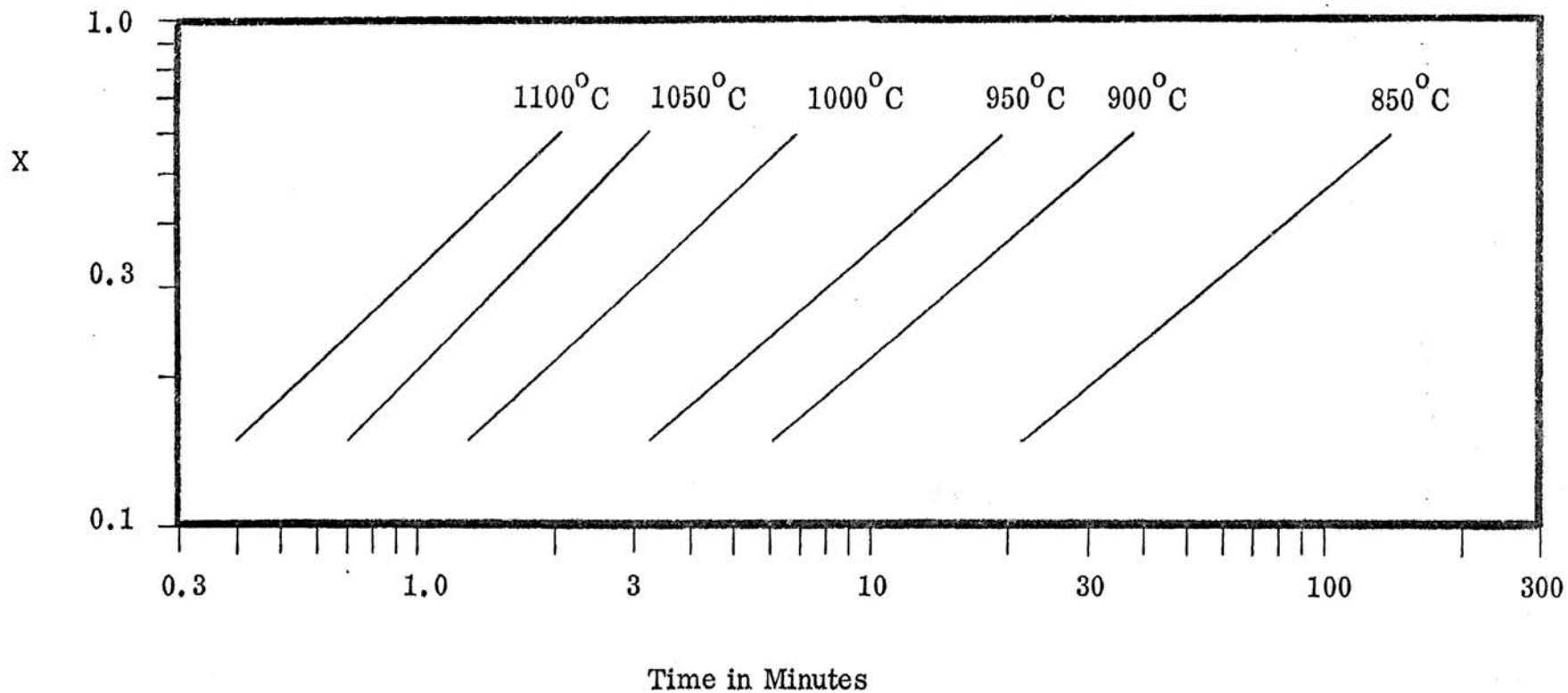
beneath the water surface, picking up the collodion film on the slide and grids when passing through the surface. When the water had dried, the copper grids were coated properly with the collodion so that the collodion film was thick enough to support the particles to be observed, yet thin enough to allow the electron beam to penetrate them.

#### IV. RESULTS

The strontium carbonate decomposition data obtained from the TGA assembly was plotted as logarithm of fraction decomposed versus logarithm time. These plots appear in Figure 2. The log-log data was analyzed by a least squares regression to determine the slope. The values of the slopes tended to increase with temperature and are tabulated in Table 1. Since they varied with respect to temperature and did not remain constant, the reciprocal of the time required for the reaction to go 50% to completion ( $t_{0.5}$ ) was used in place of the rate constant for determining activation energy.

In the Arrhenius plot in Figure 3, the natural logarithm of the reciprocal of  $t_{0.5}$  was plotted against reciprocal Kelvin temperature. The least squares regression of this curve yielded an activation energy of  $50.6 \pm 2.6$  kilocalories per mole. The analysis of variance table of this regression appears in Appendix B.

The data from the quantitative x-ray diffraction analysis of the reacted mixtures of strontium carbonate and zirconium oxide are shown in Figure 4. Each value represents the average of two determinations. They were fitted to various rate laws discussed in the literature survey to determine which rate law and corresponding model best characterized the reaction. The fraction reaction completed ( $x$ ) and time ( $t$ ) were substituted into the equations and the rate constant ( $k$ ) was calculated. These values are listed in Table 2. The rate constant was then plotted against fraction completed in Figures 5 through 10. At a particular temperature if a rate law properly describes a reaction,



FRACTION  $\text{SrCO}_3$  DECOMPOSED VERSUS TIME

Figure 2



TABLE 1

SLOPE OF PLOT OF LN FRACTION  $\text{SrCO}_3$  DECOMPOSED VERSUS LN TIMETEMPERATURE IN  $^{\circ}\text{C}$ 

	850	900	950	1000	1050	1100
1	$0.79 \pm 0.01$	$0.77 \pm 0.02$	$0.84 \pm 0.01$	$0.86 \pm 0.01$	$0.92 \pm 0.02$	$1.02 \pm 0.05$
2	$0.81 \pm 0.01$	$0.74 \pm 0.02$	$0.78 \pm 0.01$	$0.87 \pm 0.01$	$0.95 \pm 0.02$	$1.06 \pm 0.04$
3	$0.79 \pm 0.01$	$0.80 \pm 0.01$	$0.82 \pm 0.01$	$0.87 \pm 0.01$	$0.89 \pm 0.02$	$0.92 \pm 0.03$
4	$0.75 \pm 0.02$	$0.79 \pm 0.01$	$0.78 \pm 0.02$	$0.87 \pm 0.01$	$0.98 \pm 0.03$	$0.95 \pm 0.01$
5	$0.79 \pm 0.01$	$0.78 \pm 0.01$	$0.82 \pm 0.01$	$0.87 \pm 0.01$	$0.90 \pm 0.02$	$1.06 \pm 0.05$

RUN  
NUMBER

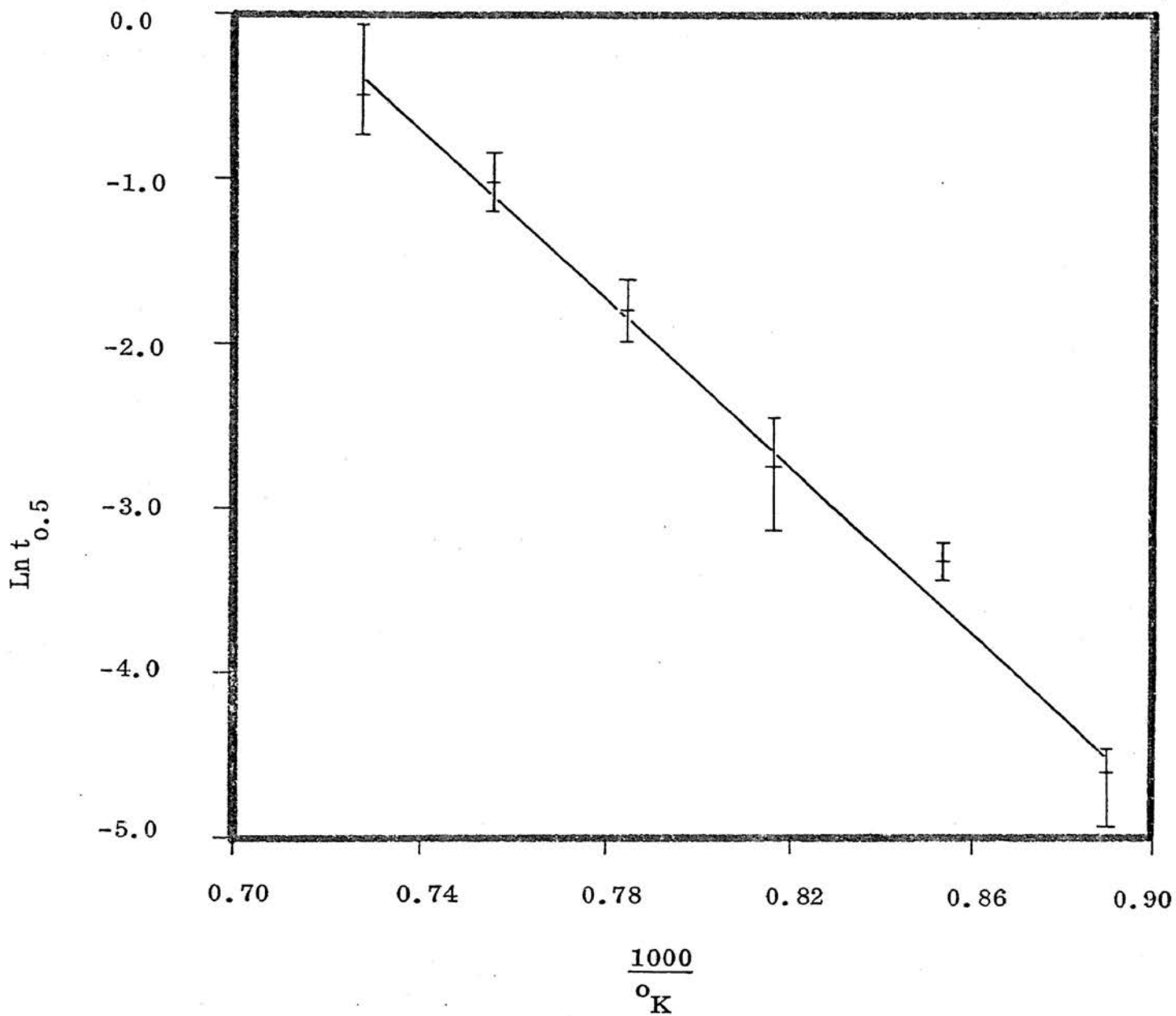
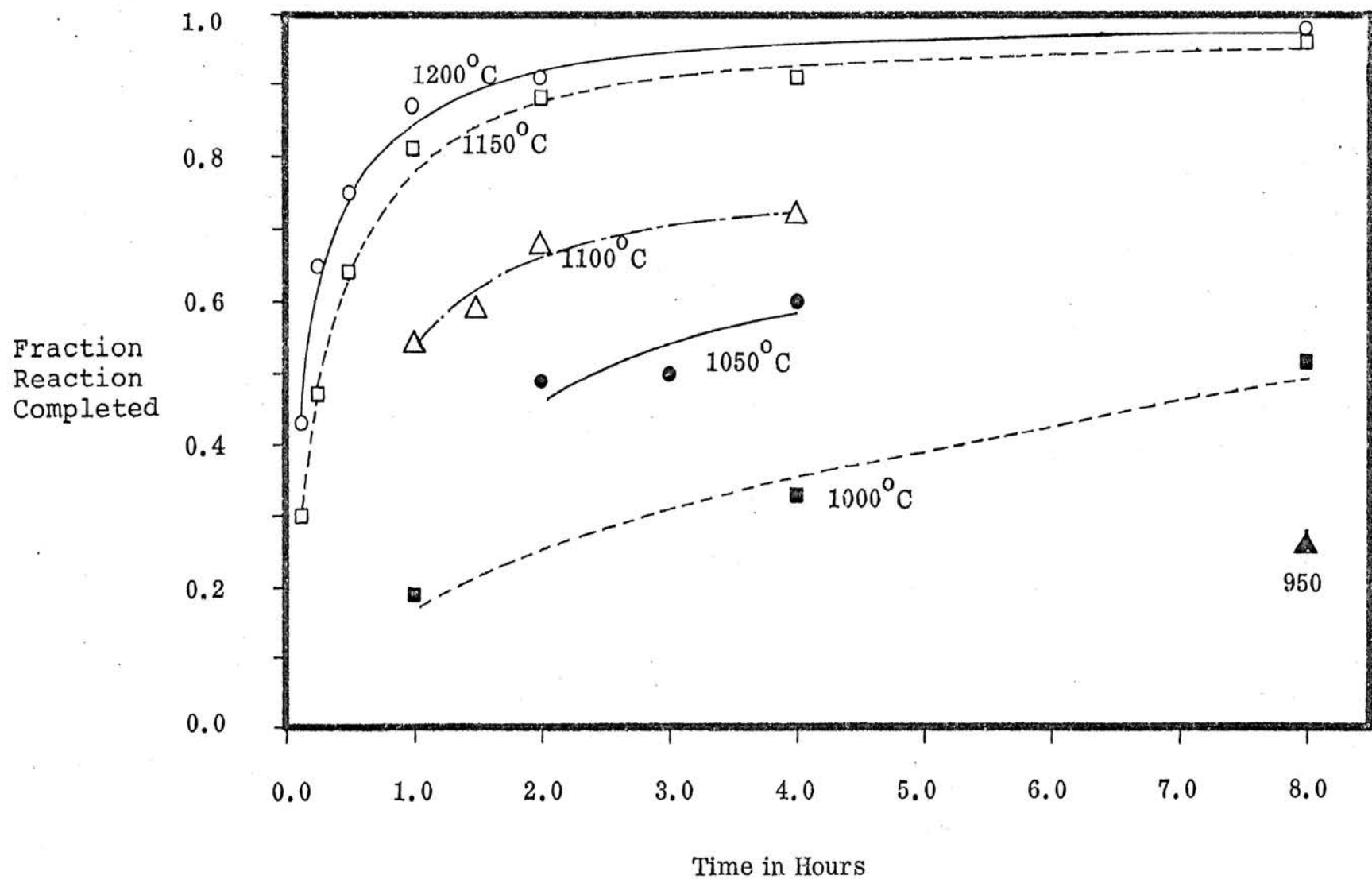
ARRHENIUS PLOT OF  $\text{SrCO}_3$  DECOMPOSITION

Figure 3



FRACTION SrZrO<sub>3</sub> FORMATION VERSUS TIME

Figure 4

TABLE 2

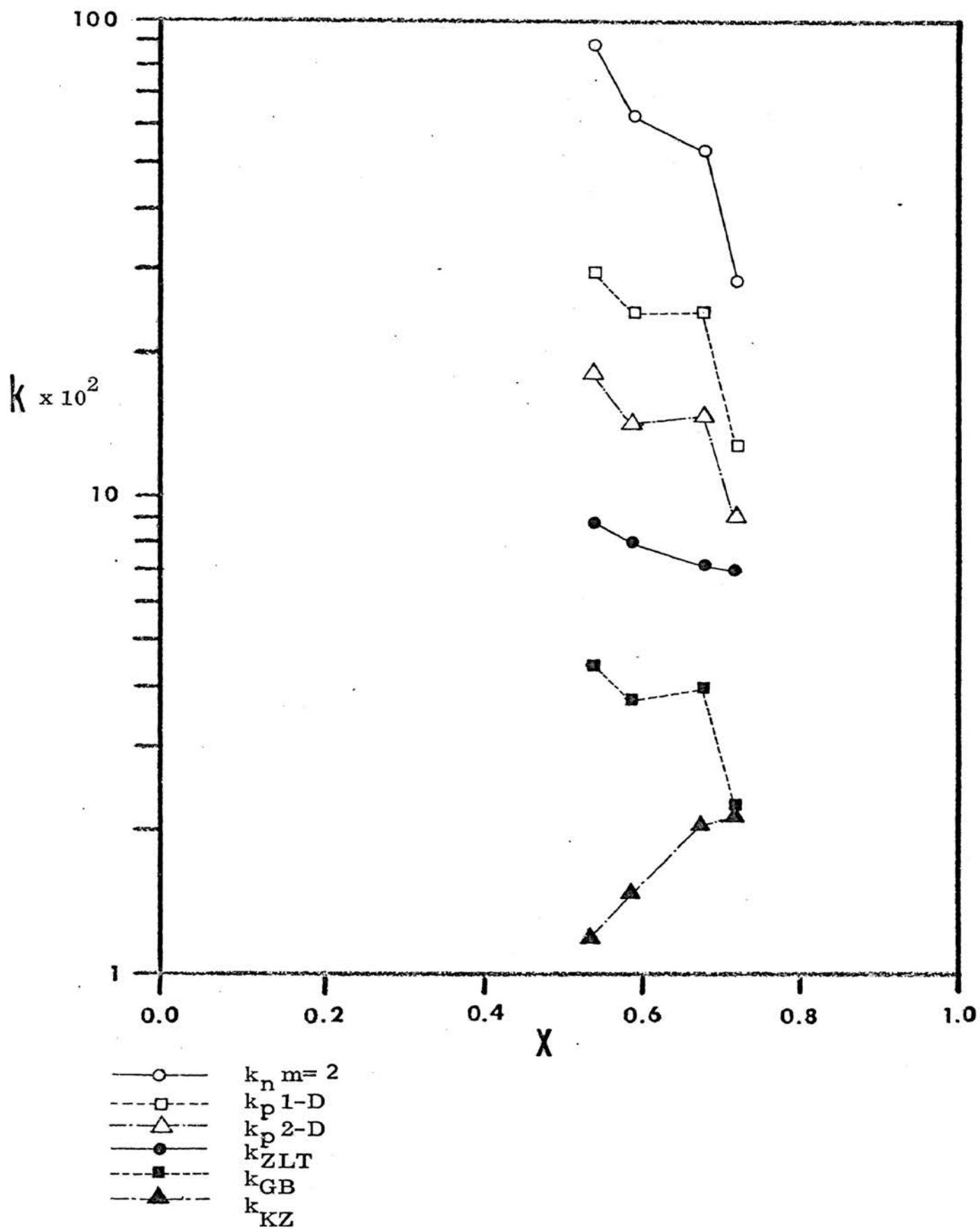
## CALCULATED RATE CONSTANTS

Temperature In °C	Fraction Reaction Completed	Time In Hours	$k_{ZLT}^{-1}$ In Hours	$k_{K-Z}^{-1}$ In Minutes	$k_{\text{parabolic}}$ 1-Dimensional In Hours <sup>-1</sup>	$k_{\text{parabolic}}$ 2-Dimensional In Hours <sup>-1</sup>	$k_J^{-1}$ In Hours
1200	0.43	0.125	0.321	0.0145	1.479	0.877	0.134
1200	0.65	0.25	0.708	0.0322	1.690	1.130	0.349
1200	0.75	0.5	0.794	0.0402	1.125	0.807	0.274
1200	0.87	1.0	0.959	0.0594	0.757	0.605	0.244
1200	0.91	2.0	0.760	0.0637	0.414	0.347	0.152
1200	0.98	8.0	0.900	0.0861	0.120	0.113	0.006
1150	0.30	0.125	0.736	0.0626	0.720	0.402	0.101
1150	0.47	0.25	0.568	0.0135	0.882	0.534	0.146
1150	0.74	0.5	0.648	0.0335	1.095	0.780	0.262
1150	0.81	1.0	0.545	0.0442	0.656	0.494	0.181
1150	0.88	2.0	0.515	0.0537	0.387	0.313	0.128
1150	0.91	4.0	0.380	0.0557	0.207	0.173	0.076
1150	0.96	8.0	0.461	0.0703	0.115	0.104	0.054
1100	0.54	1.0	0.0890	0.0127	0.292	0.183	0.0520
1100	0.59	1.5	0.0810	0.0147	0.232	0.150	0.0441
1100	0.68	2.0	0.0735	0.0209	0.231	0.158	0.0500
1100	0.72	4.0	0.0700	0.0219	0.130	0.091	0.0299
1050	0.49	2.0	0.0316	0.0308	0.1200	0.0733	0.0202
1050	0.50	3.0	0.0227	0.0126	0.0833	0.0511	0.0142
1050	0.60	4.0	0.0321	0.0082	0.0900	0.0584	0.0173
1050	0.82	8.0	0.0742	0.0069	0.0840	0.0639	0.0237
1000	0.19	1.0	0.0052	0.00115	0.0361	0.0199	0.0046
1000	0.33	4.0	0.0165	0.00266	0.0256	0.0144	0.0036
1000	0.42	8.0	0.0126	0.00338	0.0220	0.0130	0.0034
950	0.26	8.0	0.00138	0.00147	0.00845	0.0043	0.0011

TABLE 2 (CONTINUED)

## CALCULATED RATE CONSTANTS

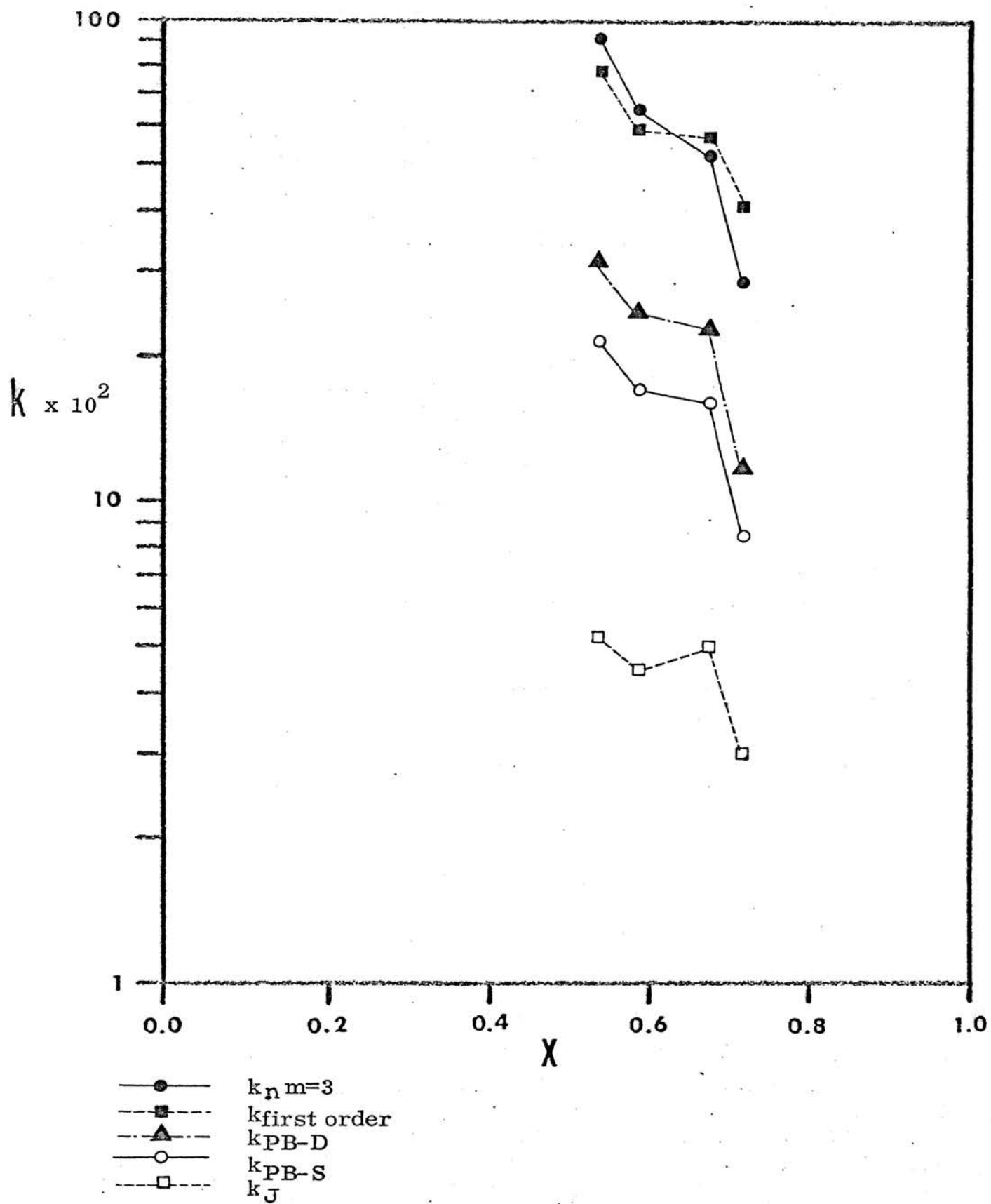
Temperature In °C	Fraction Reaction Completed	Time In Hours <sup>-1</sup>	k <sub>G-B</sub> In Hours <sup>-1</sup>	-k <sub>First Order</sub> In Hours <sup>-1</sup>	k <sub>PB-D</sub> In Hours <sup>-1</sup>	k <sub>PB-S</sub> In Hours <sup>-1</sup>	k <sub>n(m=2)</sub> In Hours <sup>-1</sup>	k <sub>n(m=3)</sub> In Hours <sup>-1</sup>
1200	0.43	0.125	0.207	4.497	1.960	1.367	5.997	6.602
1200	0.65	0.25	0.280	4.199	1.634	1.181	4.098	4.065
1200	0.75	0.5	0.206	2.773	1.000	0.740	2.356	2.236
1200	0.87	1.0	0.163	2.040	0.639	0.493	1.428	7.268
1200	0.91	2.0	0.096	1.204	0.350	0.276	0.776	0.670
1200	0.98	8.0	0.034	0.489	0.107	0.091	0.247	0.197
1150	0.30	0.125	0.0928	2.854	1.306	0.897	4.778	5.674
1150	0.47	0.25	0.127	2.540	1.088	0.763	3.187	3.438
1150	0.74	0.5	0.199	2.694	0.980	0.723	2.321	2.209
1150	0.81	1.0	0.130	1.661	0.564	0.425	1.289	1.184
1150	0.88	2.0	0.0850	1.060	0.327	0.253	0.728	0.642
1150	0.91	4.0	0.0481	0.602	0.175	0.138	0.388	0.335
1150	0.96	8.0	0.0304	0.403	0.100	0.082	0.227	0.785
1100	0.54	1.0	0.0441	0.776	0.322	0.228	0.881	0.919
1100	0.59	1.5	0.0365	0.594	0.240	0.171	0.630	0.642
1100	0.68	2.0	0.0394	0.570	0.217	0.158	0.534	0.522
1100	0.72	4.0	0.0230	0.418	0.118	0.086	0.282	0.271
1050	0.49	2.0	0.0175	0.337	0.143	0.1000	0.410	0.438
1050	0.50	3.0	0.0122	0.131	0.098	0.0688	0.278	0.295
1050	0.60	4.0	0.0143	0.229	0.092	0.0658	0.239	0.243
1050	0.82	8.0	0.0168	0.214	0.072	0.0544	0.164	0.150
1000	0.19	1.0	0.0044	0.211	0.1000	0.0678	0.459	0.595
1000	0.33	4.0	0.0034	0.096	0.0438	0.0302	0.130	0.182
1000	0.42	8.0	0.0031	0.068	0.0298	0.0208	0.092	0.102
950	0.26	8.0	0.0011	0.038	0.0175	0.0119	0.0686	0.0838



LN RATE CONSTANT VERSUS FRACTION REACTION COMPLETED

AT 1100°C

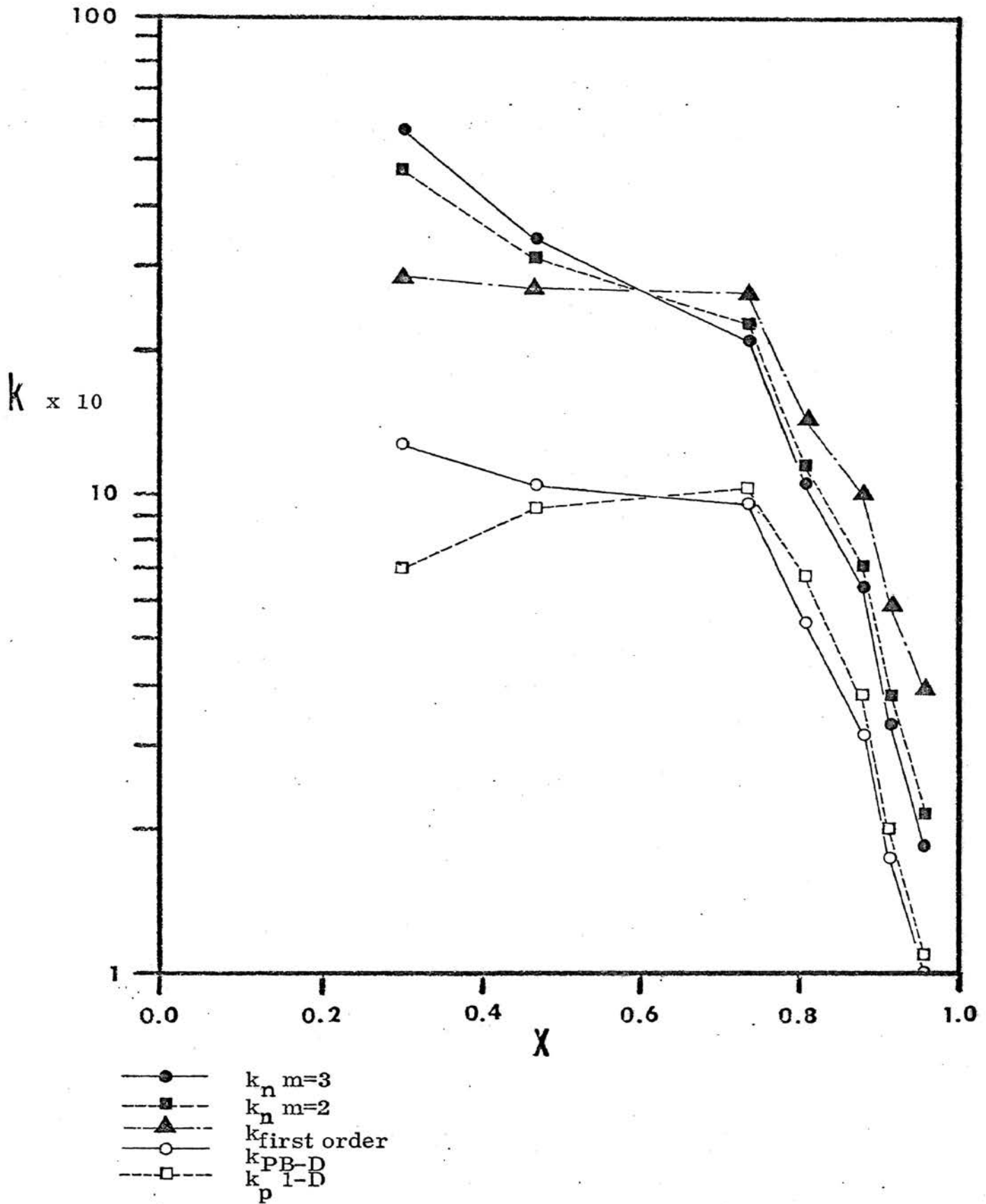
Figure 5



LN RATE CONSTANT VERSUS FRACTION REACTION COMPLETED

AT 1100°C

Figure 6

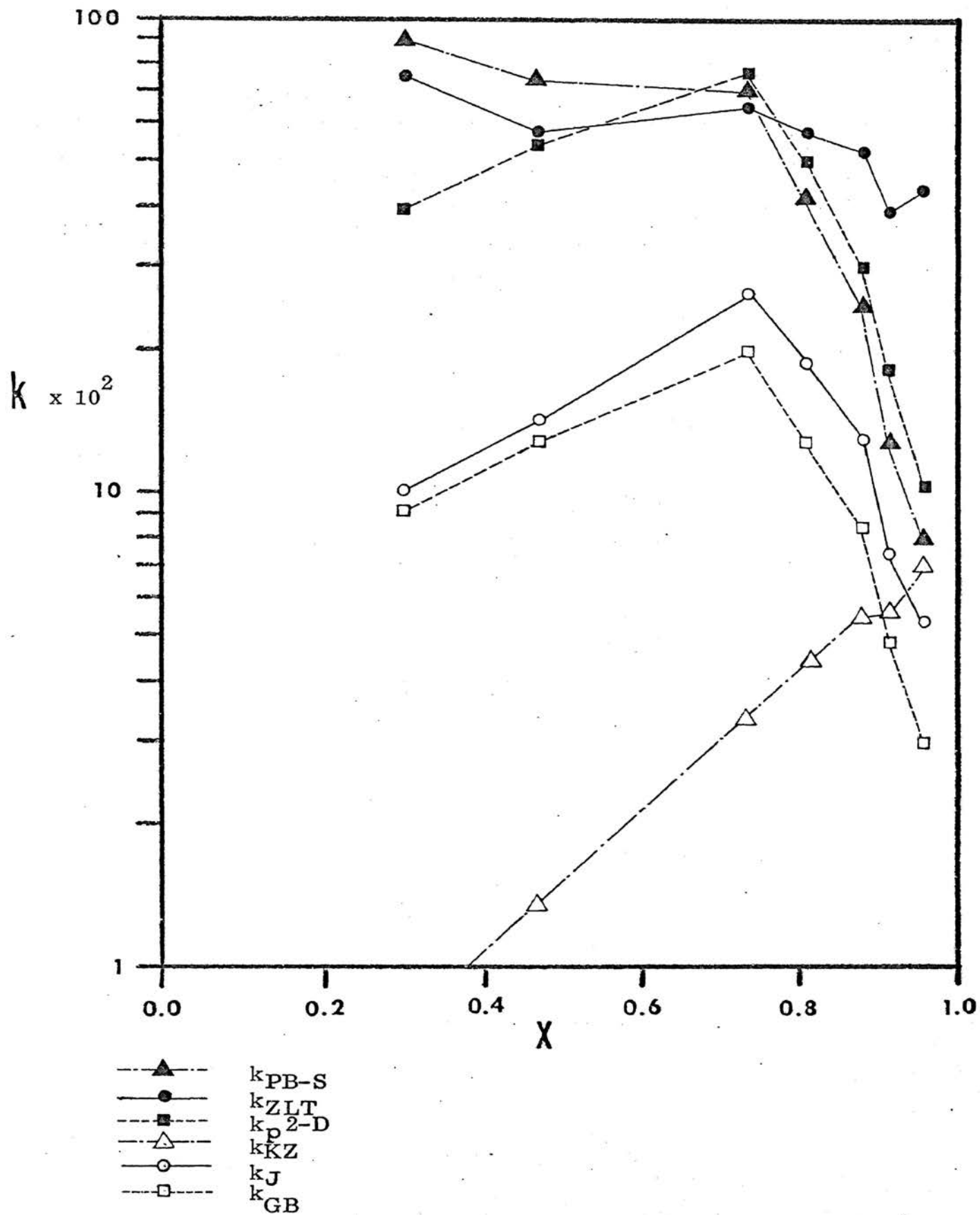


LN RATE CONSTANT VERSUS FRACTION REACTION COMPLETED

AT 1150°C

Figure 7

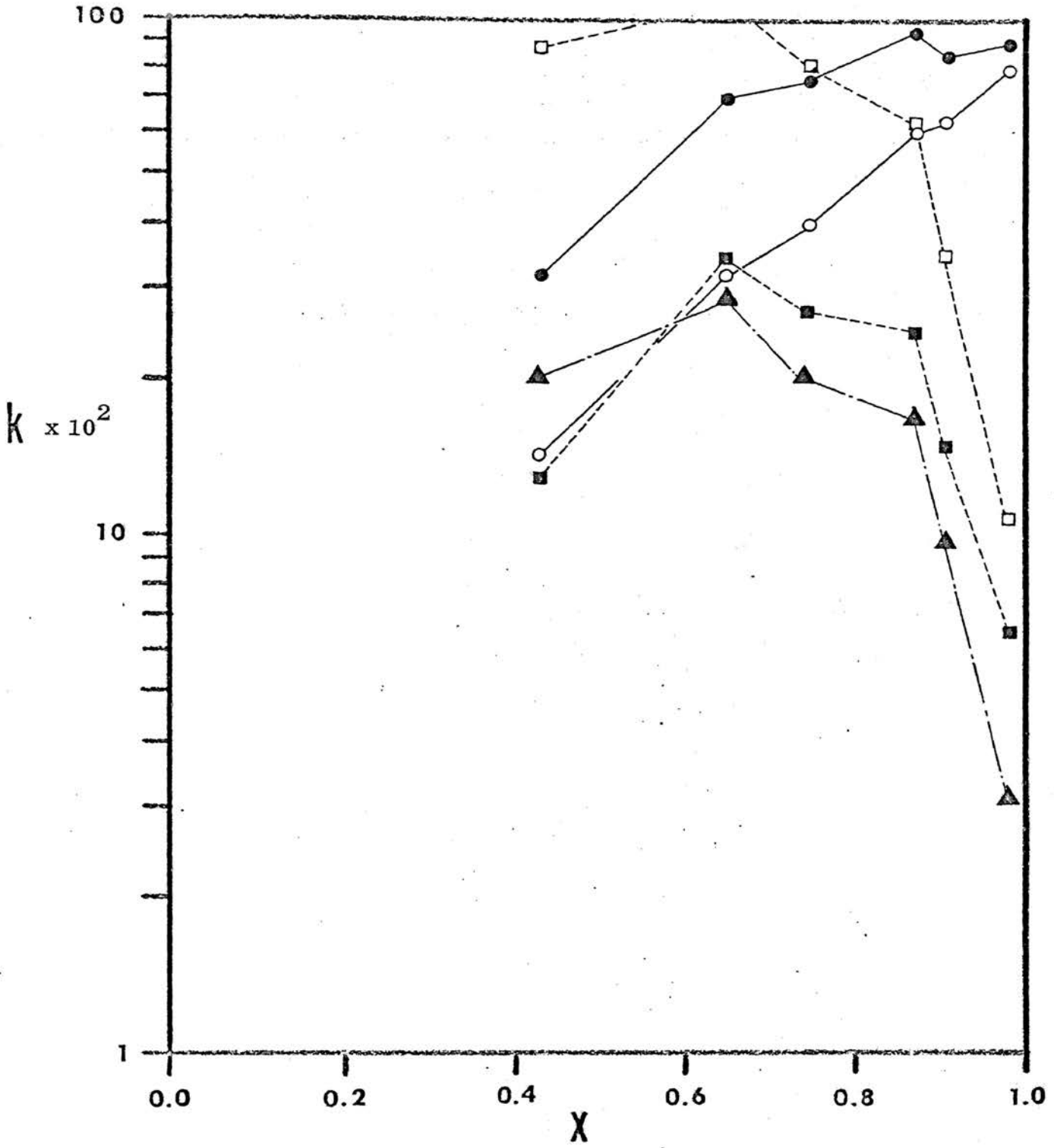




LN RATE CONSTANT VERSUS FRACTION REACTION COMPLETED

AT 1150°C

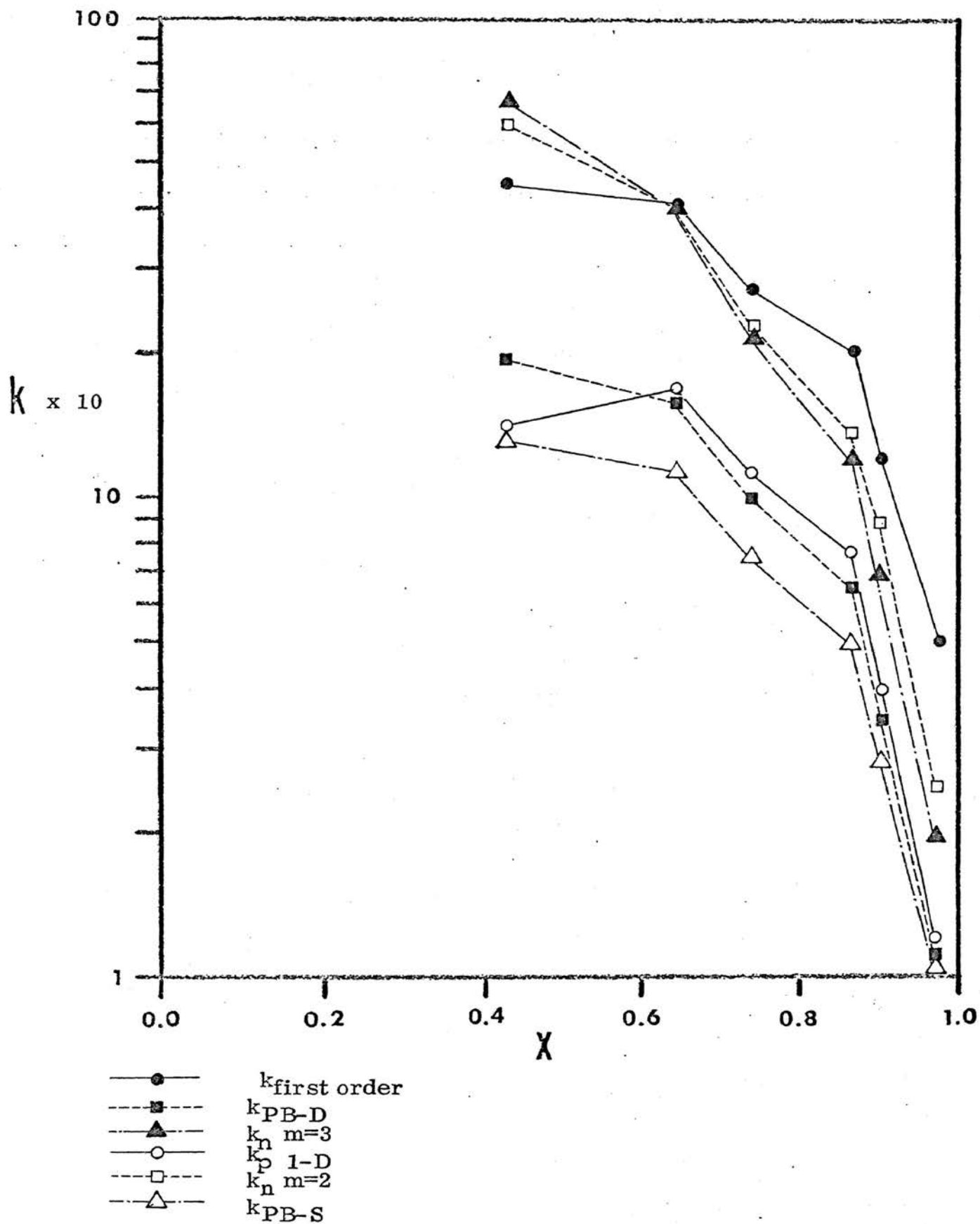
Figure 8



- $k_{ZLT}$
- -■- -  $k_J$
- -▲- -  $k_{GB}$
- $k_{KZ}$
- -□- -  $k_{p, 2-D}$

LN RATE CONSTANT VERSUS FRACTION REACTION COMPLETED  
AT  $1200^\circ\text{C}$

Figure 9



LN RATE CONSTANT VERSUS FRACTION REACTION COMPLETED

AT 1200°C

Figure 10

the rate constant, as calculated from  $x$  and  $t$ , should not vary. Since the rate constant for the Zhuravlev-Leskhin-Temple' man rate law varied less with fraction completed of the reaction its rate constant was used for the calculations of activation energy.

The Arrhenius plot of natural logarithm of rate constant versus reciprocal Kelvin temperature appears in Figure 11. A least squares regression analysis of this curve yielded an activation energy of  $81.3 \pm 9.6$  kilocalories per mole.

The analysis of variance table for the regressions of these activation energies appear in Appendix C.

The electron photomicrographs of the reacted powders appear in Appendix D. Three of these electron photomicrographs show dendritic crystals which are the result of the method used to prepare the samples for observation in the electron microscope and are not directly pertinent to this study but were included because they might be of interest.

Typical DTA curves appear in Appendix E.

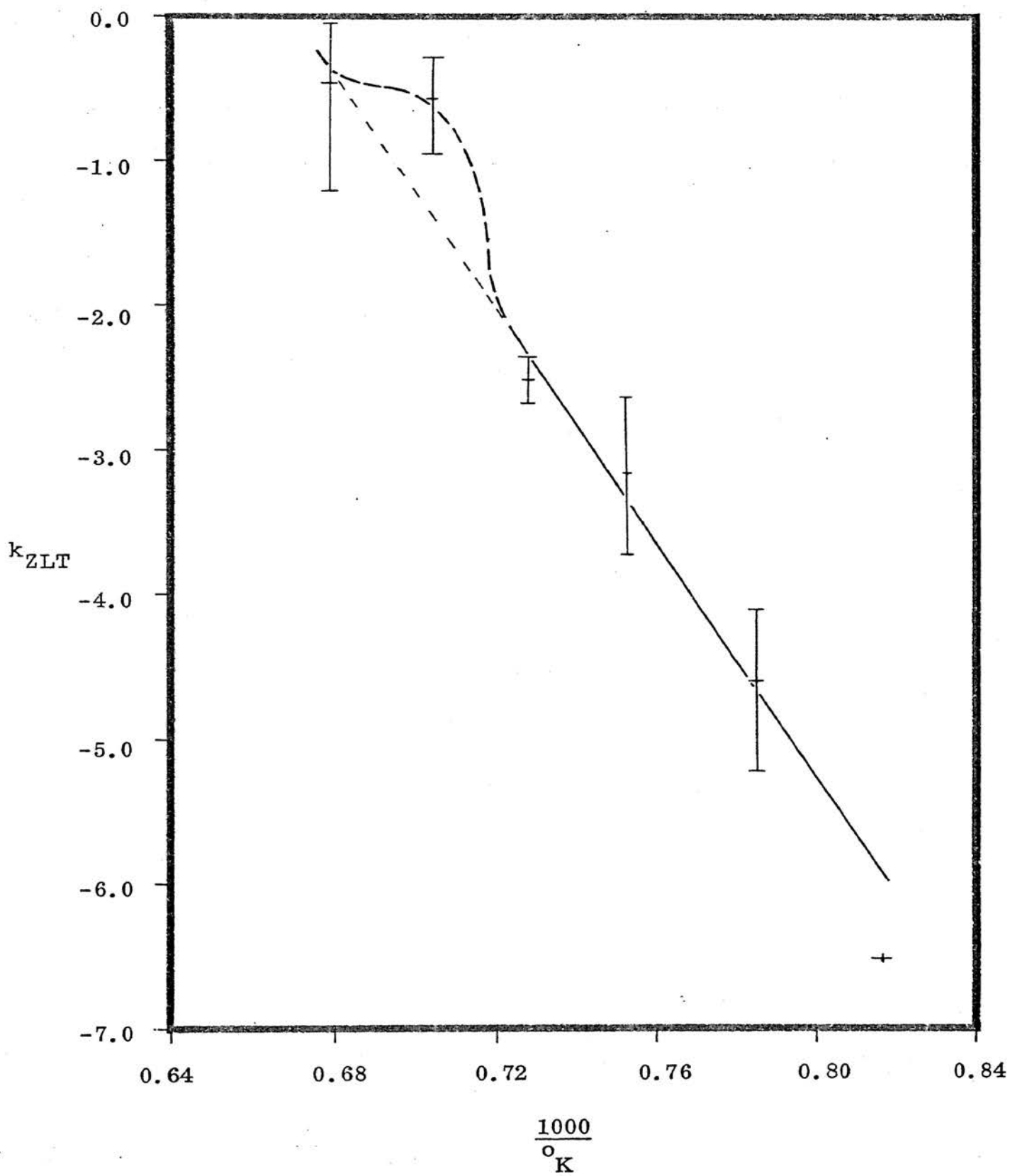
ARRHENIUS PLOT  $\text{SrZrO}_3$  FORMATION

Figure 11

## V. DISCUSSION OF RESULTS

As shown from the data, the decomposition of strontium carbonate does not follow the classical rate theory but deviates somewhat from zero-order. For the reaction to be zero order the slope on a log-log plot should be one. The calculated slopes ranged from 0.74 to 1.06. It is possible that these deviations from 1.0 are caused by a distribution of particle sizes and would be minimized if a single particle size were used. Classical rate theory is generally not considered to fit solid state reactions to the extent that it fits many liquid and gaseous reactions. A set of rate constants ( $k_c$ ), based on equations of the type,

$$x = k_c t^\sigma \quad (15)$$

where  $\sigma$  is the slope of the log-log plot, would not be equivalent if  $\sigma$  is not constant. For this reason, the reciprocal of the time required for the reaction to reach one-half of completion is a better value to use for an Arrhenius plot as in Figure 3.<sup>14</sup> The activation energy found from this plot is  $50.6 \pm 2.6$  kilocalories per mole. Wanmaker and Radielovic<sup>31</sup> reported an activation energy of  $55 \pm 3$  kilocalories per mole. These values are both quite near the value of the heat of decomposition of 56 kilocalories per mole. While an activation energy of decomposition and heat of decomposition cannot be directly related to each other, it has been suggested by Garner<sup>32</sup> that when they are equal, as is often the case with carbonates and hydroxides, the decomposition reaction is analogous to the evaporation of a liquid.

The entropy of activation, calculated by the method discussed by Branson,<sup>13</sup> was found to be  $-71$  e.u. This large and negative value of entropy of activation is indicative of an activated complex which is relatively complicated as compared to the reactant.

From x-ray diffraction and TGA data, it was determined that the rate of decomposition of the strontium carbonate is faster than the rate of formation of  $\text{SrZrO}_3$ . This can be seen by comparing Figures 2 and 4. This behavior was first observed when a mixture of strontium carbonate and zirconium oxide was used as a sample in the TGA apparatus. After the sample showed total decomposition of the strontium carbonate and was removed from the furnace, it gained weight. It was assumed that this represented the absorption of water by the unreacted strontium oxide. An x-ray pattern of the same sample showed unreacted zirconium oxide to be present also. This disallowed the use of the TGA apparatus in following the combination reaction between strontium carbonate and zirconium oxide and also showed that the actual reaction is between strontium oxide and zirconium oxide.

The plots of logarithm of rate constant versus fraction reaction completed (Figures 5 through 10) were made to determine which of the models discussed in the literature survey is most suited to the combination reaction rate data. In general the nucleation, phase boundary, and classical first order calculated rate constants show a decrease with increasing fraction reaction completed, especially above  $x = 0.5$ . The Ginstling-Brounshtein and Jander calculated rate constants tend to have a maximum at about  $x = 0.6$  to  $0.7$  and fall off at

both higher and lower values of  $x$ . The Kroger-Ziegler calculated rate constant appears to increase with  $x$  and has an almost constant slope on the semi-log plot. The Zhuravlev-Lesokhin-Tempel' man rate constant is shown to have less variation with changes in  $x$  and is assumed to be the best fit. The Carter and Valensi rate constants could not be calculated since there is no data available on the high temperature density of strontium zirconate.

As the Zhuravlev-Lesokhin-Tempel' man rate equation was chosen as most nearly fitting the reaction rate data, it is also assumed that the corresponding model describes the mechanism of the reaction. This indicates that the reaction rate is diffusion controlled and that the activity of the reactants is not constant but decreases as the reaction proceeds. It should, however, be noted that the data used is all above  $x = 0.19$  and generally above  $x = 0.4$ .

Branson<sup>13</sup> has shown that while most of a reaction may be diffusion controlled, the initial part of the reaction may be controlled by some other process. This could not be determined in this reaction because of the effect of the incomplete decomposition of the strontium carbonate on the complex x-ray pattern.

The Zhuravlev-Lesokhin-Tempel' man rate constants were used in the Arrhenius plot in Figure 11. The activation energy was found to be  $81.3 \pm 9.7$  kilocalories per mole. Hulbert and Popowich<sup>33</sup> report activation energies of 66.6 and 97.8 kilocalories per mole for the reactions between strontium carbonate and anatase and between strontium carbonate and rutile respectively.

This activation energy, as found, could result from one or a combination of any of the reactions or processes below:



- a.  $\text{ZrO}_2 + n\text{SrO} \rightarrow (\text{ZrO}_2 \cdot n\text{SrO})_{\text{SS}} (\text{Stabilized ZrO}_2)$
- b.  $(\text{ZrO}_2 \cdot n\text{SrO})_{\text{SS}} (\text{Stabilized ZrO}_2) + (1 - n)\text{SrO} \rightarrow \text{SrZrO}_3$
- c.  $\text{SrO} + \text{ZrO}_2 \rightarrow \text{SrZrO}_3$
- d. Diffusion of  $\text{Zr}^{+4}$ ,  $\text{Sr}^{+2}$ ,  $\text{O}^{-2}$ , SrO or  $\text{ZrO}_2$   
through the  $\text{SrZrO}_3$  product layer.

Since the reaction appears to be diffusion controlled, it could be assumed that this activation energy would be for the diffusion process, or at least closely associated with the activation energy of the diffusion process. If the reaction had been found to be phase boundary or nucleation controlled, the activation energy would be expected to be that of one of the chemical combination reactions or at least closely related.

The hump shown in the Arrhenius plot occurs around the transformation temperature for zirconia. This type behavior, first reported by Hedvall,<sup>34</sup> is found quite often and is referred to as the "Hedvall Effect". The Hedvall effect can result in a hump or a discontinuity in an Arrhenius plot. If it shows a discontinuity, a different activation energy above and below the transformation temperature should exist. The reason for this hump is the increased reactivity of the zirconia while undergoing the crystallographic transformation. In a diffusion controlled reaction, any one of the migrating species might be the rate limiting species. In the case of this reaction the migrating species would be  $\text{Sr}^{+2}$ ,  $\text{Zr}^{+4}$ , and  $\text{O}^{-2}$ , as the migrating species are ions. At the transformation temperature where one of the reactants is more reactive, this would affect the freeing of more ions to migrate but would not increase their rate of

diffusion. Here the reaction rate should return to follow the Arrhenius plot. If the reaction were phase boundary or nucleation controlled this would probably not be the case and a break or discontinuity in the Arrhenius plot would be expected.

The entropy of activation was calculated to be  $-71$  e.u. This is the same as the value obtained for the decomposition of the strontium carbonate. It is possible that the similarity in magnitude of the entropy of activation terms may be indicative of a similar activated complex. An obvious conclusion from this might be that the activated complex is a very open strontium oxide into which the zirconium atoms could travel and position themselves such that the step down to the perovskite type structure could be spontaneous.

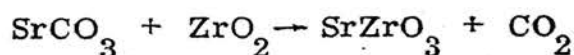
## VI. CONCLUSIONS

1. The decomposition of strontium carbonate deviates slightly from a classical zero-order reaction and has an activation energy of  $50.6 \pm 2.6$  kilocalories per mole.
2. The decomposition of strontium carbonate is more rapid than the formation of strontium zirconate; thus, the strontium oxide formed from this decomposition is the material which is reacting with the zirconium oxide.
3. The formation of strontium zirconate from zirconium oxide and the decomposition product of strontium carbonate appears to be diffusion controlled and most nearly follows the Zhuravlev-Lesokhin-Tempel<sup>r</sup> man rate equation of  $k_{ZLT} t = \left[ \frac{1}{1-x} \right]^{1/3} - 1 \Big]^2$
4. The apparent activation energy for the formation of strontium zirconate from zirconium oxide and the decomposition product of strontium carbonate is  $81.3 \pm 9.7$  kilocalories per mole.
5. The reaction rate exhibits a non-linear increase at or about the transformation temperature of the zirconium oxide and thus illustrates the Hedvall effect.

## VII. SUGGESTIONS FOR FUTURE WORK

During the course of this investigation several interesting questions appeared which could not be investigated fully. These were mainly concerned with determination of the detailed mechanism of the formation of strontium zirconate and the variations in the rate of formation of strontium zirconate in the vicinity of the zirconia inversion. A list of these suggestions for future work with some suggested avenues of approach follow:

1. Study the diffusion of  $\text{Sr}^{+2}$ ,  $\text{Zr}^{+4}$ ,  $\text{O}^{-2}$ ,  $\text{SrO}$  and  $\text{ZrO}_2$  in  $\text{SrZrO}_3$  to determine which possible migrating species might be the rate limiting specie. This might be possible by making diffusion couples and using radioactive tracer techniques.
2. Study the magnitude of the formation of the stabilized zirconia phase and attempt to determine the role it might play in the formation of  $\text{SrZrO}_3$ . This might be possible by the use of hot stage x-ray diffraction.
3. Examine the rate of formation of  $\text{SrZrO}_3$  in more detail around the zirconia inversion temperature to better determine the magnitude to which it affects the reaction rate and illustrates the Hedvall effect.
4. Study the effect of  $\text{CO}_2$  pressure on the decomposition of  $\text{SrCO}_3$  and the formation of  $\text{SrZrO}_3$  to determine if at some  $\text{CO}_2$  pressure the actual reaction might be



such that better kinetic data might be taken on a TGA apparatus.

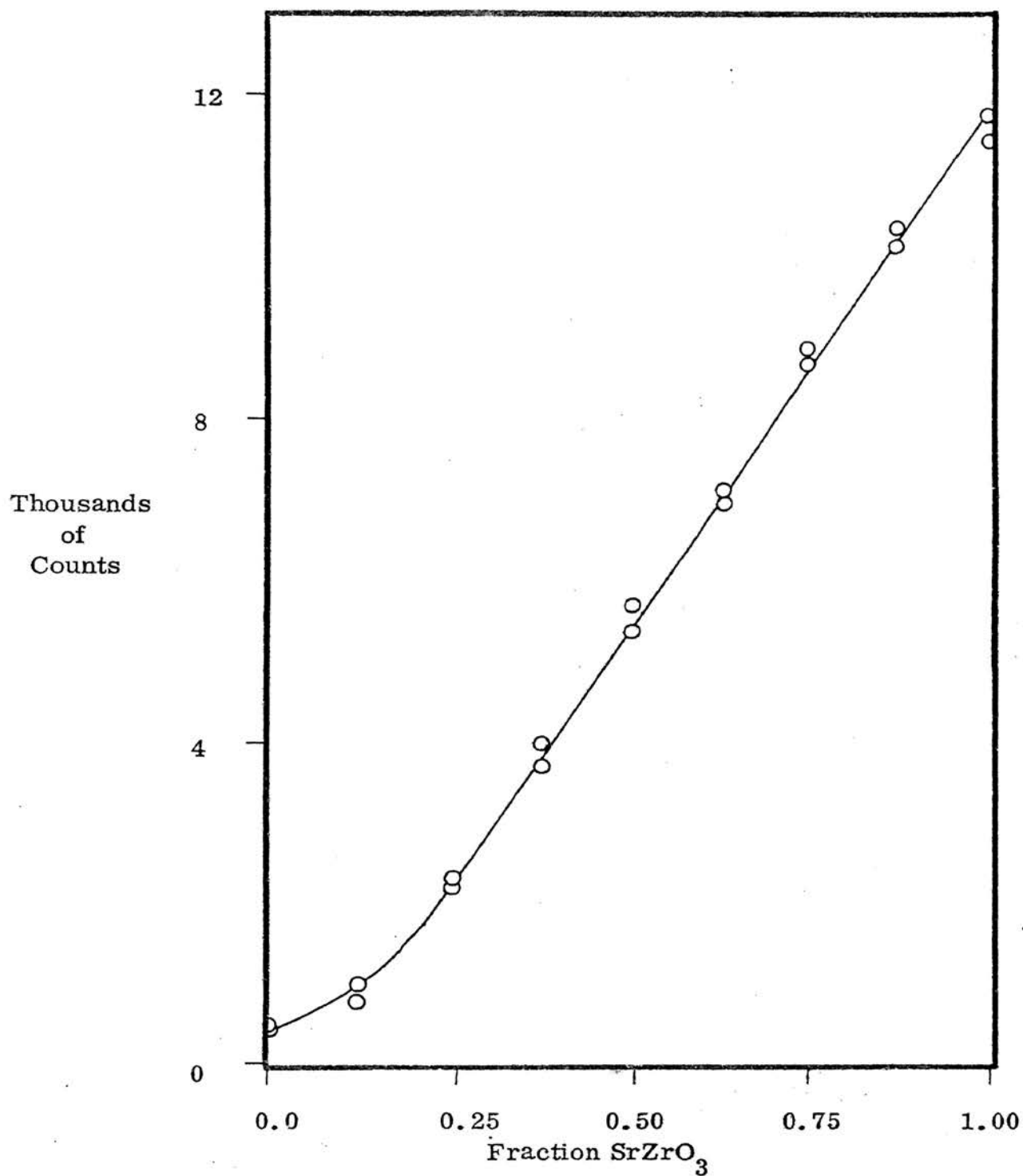
## BIBLIOGRAPHY

1. W. Jander, "Reactions in Solid State at High Temperatures, I," *Z. Anorg. Allgem. Chem.*, 163 (1-2), 1-30 (1927).
2. C. Kroger and G. Ziegler, "Reaction Rates of Glass Batch Melting, II," *Glastech. Ber.* 26 (11) 346-53 (1953).
3. C. Kroger and G. Ziegler, "Reaction Rates of Glass Batch Melting, III," *ibid.*, 27 (6) 199-212 (1954).
4. V. F. Zhuravlev, I. G. Lesokhin, R. G. Tempel'man, "Kinetics of the Reactions for the Formation of Aluminates and the Role of Mineralizers in the Process," *J. Appl. Chem. USSR (English Translation)* 21 (9) 887-902 (1948).
5. A. M. Ginstling and B. I. Brounshtein, "Concerning the Diffusion Kinetics of Reactions in Spherical Particles," *J. Appl. Chem. USSR (English Translation)* 23, 1327-38 (1950).
6. P. M. Barrer, "Diffusion in Spherical Shells, and a New Method of Measuring the Thermal Diffusivity Constant," *Phil. Mag.* 35 (12) 802-11 (1944).
7. R. E. Carter, "Kinetic Model for Solid State Reactions," *J. Chem. Phys.* 34 (6) 2010-15 (1961).
8. R. E. Carter, "Addendum: Kinetic Model for Solid State Reactions," *ibid.*, 35 (3) 1137-38 (1961).
9. G. Valensi, "Kinetics of the Oxidation of Metallic Spherules and Powders," *Compt. Rend.*, 202 (4) 309-12 (1936).
10. H. Dunwald and C. Wagner, "Measurement of Diffusion Rate in the Process of Dissolving Gases in Solid Phases," *Z. Physik, Chem. (Leipzig)* B24 (1) 53-58 (1934).
11. B. Serin and R. T. Ellickson, "Determination of Diffusion Coefficients," *J. Chem. Phys.* 9, 742-47 (1941).
12. E. A. Geiss, "Equations and Tables for Analyzing Solid State Reaction Kinetics," *Jour. Am. Cer. Soc.* 46 (8) 374-76 (1963).
13. D. L. Branson, "Kinetics of Zinc Aluminate Spinel Formation," Ph.D. Dissertation, Ohio State University, Columbus, Ohio (1964).

14. W. W. Pultz and W. Hertl, "Oxidation of Particulate Silicon Monoxide," *Journ. Am. Cer. Soc.* 50 (4) 202-203 (1967).
15. S. Miyagi, "A Criticism on Jander's Equation of Reaction Rate Considering the Statistical Distribution of Particle Size of Reacting Substance," *J. Japan Cer. Soc.*, 59, 132-35 (1951).
16. H. Sasaki, "Introduction of Particle Size Distribution into Kinetics of Solid State Reactions," *Jour. Am. Cer. Soc.* 47 (10) 512-16 (1964).
17. H. J. Gallagher, "The Effect of Particle Size Distribution on the Kinetics of Diffusion Reactions in Powders," *Reactivity of Solids*, edited by G. M Schwab, 192-203, Elsevier Publishing Company, New York (1965).
18. W. Komotsu, "The Kinetic Equation of the Solid State Reaction: The Effect of Particle Size and Mixing Ratio on the Reaction Rate in a Mixed Powder System," *ibid.* 182-91.
19. A. F. E. Welch, "Solid - Solid Reaction," *Solid State Chemistry*, edited by W. E. Garner, 297-310, Butterworths, London, Scientific Publications (1953).
20. P. W. M. Jacobs and F. C. Tompkins, "Classifications and Theory of Solid Reactions," *ibid.*, 184-211.
21. M. E. Fine, *Phase Transformations in Condensed Systems*, 47-78, MacMillan Co. (1964).
22. M. Avrami, "Kinetics of Phase Change," *J. Chem. Phys.* 7, 1103-12 (1939).
23. *Ibid.*, 8, 212-24 (1940).
24. *Ibid.*, 9, 177-84 (1941).
25. B. V. Erofe'ev, "Generalized Equations of Chemical Kinetics and Its Application in Reactions Involving Solids," *Compt, Rend. Acad. Sci. USSR*, 52, 511-14.
26. J. W. Christian, *The Theory of Transformations in Metals and Alloys*, 471-95, Pergoman Press, New York (1965).
27. K. J. Laidler, *Chemical Kinetics*, 316-318, McGraw-Hill Inc., New York (1965).

28. J. H. Sharp, G. W. Brindley, and B.N. Narahari Achar, "Numerical Data for Some Commonly Used Solid State Reaction Equations," *J. Am. Cer. Soc.* 49 (7), 379-82 (1966).
29. A. Bielanski, J. Nedoma, W. Turowa, "Studies on the Polymorphic Transformations of Sodium Fluoroberyllate," pp 90-99, Reactivity of Solids, edited by G. M. Schwab, Elsevier Publishing Company, New York 1965.
30. E. V. Garner, "The Powder Method in the Industrial Chemical Laboratory," pp 510, X-Ray Diffraction by Polycrystalline Materials, edited by H. S. Peiser, H. P. Rooksby and A. J. C. Wilson, The Institute of Physics, London 1955.
31. W. L. Wanmaker and D. Radielovic, "The Dependence of the Rate of the Dissociation of Strontium Carbonate in Some Mixtures on Particle Size and Composition," p 529, Reactivity of Solids, edited by G. M. Schwab, Elsevier Publishing Company, New York 1965.
32. W. E. Garner, *Chemistry of the Solid State*, pp 213-53, edited by W. E. Garner, Butterworths Scientific Publications, London, 1955.
33. S. F. Hulbert and M. J. Popowich, "Kinetics and Mechanism of the Reaction Between  $\text{TiO}_2$  and  $\text{SrCO}_3$ ", Paper presented at International Symposium on Ceramics, Alfred, N. Y., June 1967.
34. J. A. Hedvall, *Reactions Fahigkeit Fester Stoffe*, Leipzig, 1938.

APPENDIX A  
X-RAY DIFFRACTION CALIBRATION CURVE



X-RAY DIFFRACTION CALIBRATION CURVE

Figure A-1



APPENDIX B

ANALYSIS OF VARIANCE OF LINEAR REGRESSION OF ARRHENIUS

PLOT FOR DECOMPOSITION OF STRONTIUM CARBONATE

Source of Variation	Degrees of Freedom	Sum of Squares	Variance Mean Squares	Calculated F-Ratio	Expected Mean Squares	Significance
Linear Regression	1	60.097125	60.097125	1126.344	$\sigma^2 + 0.092\beta^2$	$\alpha < 0.0005$
Lack of Fit	4	0.557164	0.139291	3.571	$\sigma^2 + k\sigma_{LOF}^2$	$\alpha = 0.02$
Experimental Error	24	0.93680096	0.039033373	----	$\sigma^2$	---
(Residual)	(28)	1.493965	0.05335589	----	$\sigma^2$ (pooled)	---
Total	29	61.59109				

Equation  $\ln \frac{1}{t_{0.5}} = -18.22 + 25.56 \left( -\frac{1}{T} \right)$

Explains 97.6% of the observed total variation in  $\ln \frac{1}{t_{0.5}}$  at the 99.95% confidence level.

APPENDIX C

ANALYSIS OF VARIANCE OF LINEAR REGRESSION OF ARRHENIUS

PLOT FOR FORMATION OF STRONTIUM ZIRCONATE

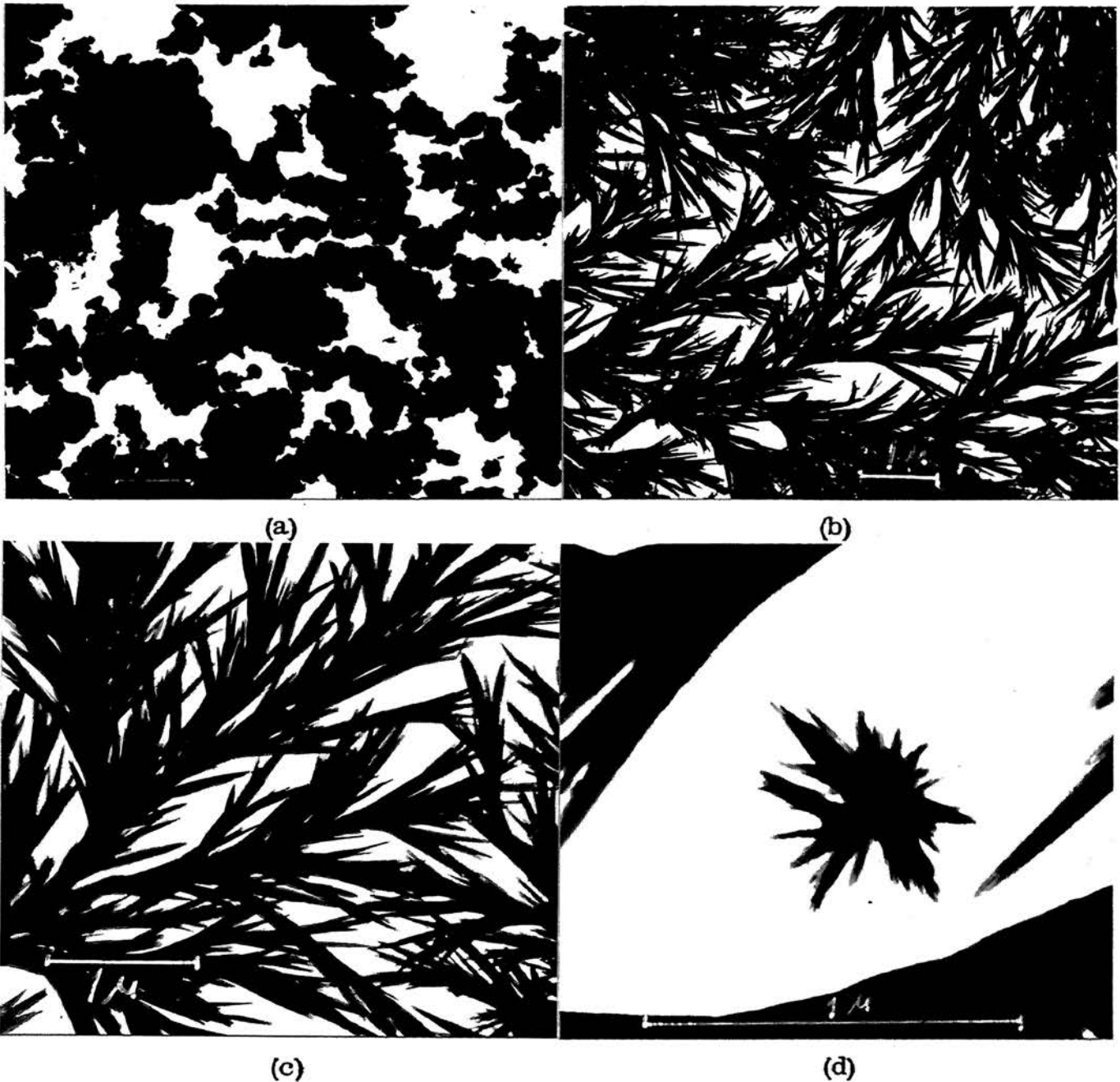
Source of Variation	Degrees of Freedom	Sum of Squares	Variance Mean Squares	Calculated F-Ratio	Expected Mean Squares	Significance
Linear Regression	1	58.84449	58.84949	350	$\sigma^2 + 0.035\beta$	$\alpha < 0.0005$
Lack of Fit	3	0.66250	0.22083	1.19	$\sigma^2 + k\sigma_{LOF}^2$	$\alpha = 0.40$
Experimental Error	13	2.42063	0.18620	---	$\sigma^2$	---
(Residual)	(16)	(3.08313)	0.19270	---	$\sigma^2$ (pooled)	---
Total	17	61.93262				

Equation  $\ln k_{ZLT} = -27.53 + 41.08 \left( -\frac{1}{T} \right)$

Explains 95.0% of the observed total variation in  $\ln k_{ZLT}$  at the 99.95% confidence level.

## APPENDIX D

## ELECTRON PHOTOMICROGRAPHS OF REACTED POWDERS

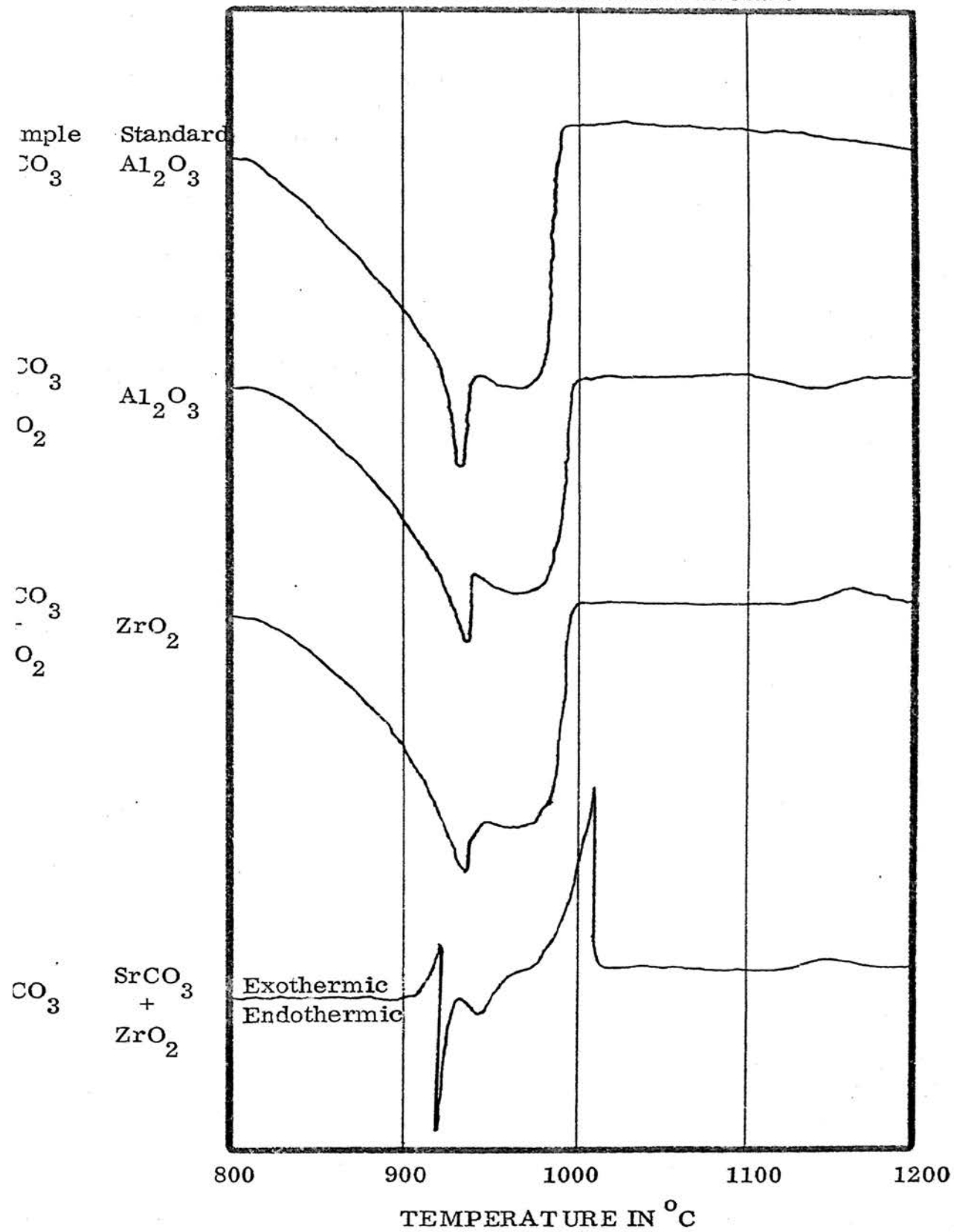


- (a) Dark areas represent strontium zirconate particles. In this sample, fired one hour at  $1200^{\circ}\text{C}$ , the reaction had gone 87% to completion. (10,000 x)
- (b) Dark dendritic areas represent strontium hydroxide formed in the preparation of the samples for the electron photomicrographs. In this sample, fired 8 hours at  $950^{\circ}\text{C}$ , the reaction had gone 26% to completion. (10,000 x)
- (c) Same sample as (b) (20,000 x)
- (d) Same sample as (b) (50,000 x)

Figure D-1

## APPENDIX E

## DIFFERENTIAL THERMAL ANALYSIS FIGURES



TEMPERATURE IN °C

DTA PLOTS

Figure E-1

## VITA

William H. Parker was born in Phelps County, Missouri on March 24, 1941. He received his elementary and secondary education from Rolla Public Schools, Rolla, Missouri. In May of 1963 he received his Bachelor of Science Degree in Ceramic Engineering from the University of Missouri School of Mines and Metallurgy (University of Missouri-Rolla), Rolla, Missouri. He worked for over two years for Armco Steel Corporation, Research and Technology Laboratory, Middletown, Ohio. While working toward his Master of Science Degree he was the recipient of the Kaiser Refractories Fellowship.

132094